Available online at www.sciencedirect.com
ScienceDirect
C. R. Physique 9 (2008) 110–118
COMPTES RENDUS PHYSIQUE
http://france.elsevier.com/direct/COMREN/

New concepts for nanophotonics and nano-electronics

Hybrid bulk heterojunction solar cells based on blends of TiO_2 nanorods and P3HT

Johann Bouclé [a,b,*], Sabina Chyla [c], Milo S.P. Shaffer [c], James R. Durrant [c], Donal D.C. Bradley [a], Jenny Nelson [a]

[a] *Department of Physics, Blackett Laboratory, Imperial College London, London SW7 2BW, United Kingdom*
[b] *Cavendish Laboratory, Madingley Road, Cambridge, CB3 0HE, United Kingdom*
[c] *Department of Chemistry, Imperial College London, London SW7 2AZ, United Kingdom*

Available online 12 February 2008

Abstract

Over the past decades, organic solar cells based on semiconducting polymers or small molecules have become a promising alternative to traditional inorganic photovoltaic devices. However, to address the intrinsic limitations of organic materials, such as charge separation yield, charge transport and durability, new strategies based on hybrid organic/inorganic materials have been explored. One such approach exploits mesoporous inorganic nanostructures as electron acceptors, which takes advantage of the potential to control the active layer structure and interface morphology through nanoparticle synthesis and processing. In this work, the potential of hybrid photovoltaics will be discussed and illustrated through a recent study of bulk heterojunction systems based on the blend of TiO_2 nanorods with a conjugated polymer. ***To cite this article: J. Bouclé et al., C. R. Physique 9 (2008).***

Résumé

Cellules solaires à hétérojonction à base de nanofils de TiO_2 et de P3HT. Depuis plus de deux décennies, les cellules solaires organiques basées sur l'utilisation de molécules ou de polymères semi-conducteurs ont démontré de fortes potentialités. Néanmoins, et pour répondre aux limitations intrinsèques dues aux matériaux organiques (nature de l'exciton, durée de vie limitée, etc.), de nouvelles stratégies de composants hybrides basés sur l'association de matériaux organiques et inorganiques ont vu le jour. Ces nouvelles approches, basées sur l'utilisation de couches mésoporeuses inorganiques ou de nanocristaux semi-conducteurs accepteurs d'électrons, permettent en particulier un contrôle fin des architectures et des interfaces à l'échelle nanométrique. Dans ce contexte, ce travail a pour objectif la description des potentialités des composants hybrides pour la conversion photovoltaïque en s'appuyant sur un exemple récent de cellule à hétérojonction basée sur le mélange de nanofils de TiO_2 avec un polymère conjugué. ***Pour citer cet article : J. Bouclé et al., C. R. Physique 9 (2008).***

Keywords: Bulk-heterojunction; Hybrid; Solar cells; Conjugated polymers; P3HT Semiconducting nanocrystals; TiO_2

Mots-clés : Cellules solaires à heterojunction ; Composants hybrides ; Polymère conjugués ; P3HT ; Nanocristaux semi-conducteurs ; TiO_2

* Correspondence to: XLIM-Minacom, UMR CNRS 6172, Optoélectronique Plastique, Faculté des Sciences et Techniques, 123 Avenue Albert Thomas, 87060 Limoges Cedex, France. Department of Physics, Blackett Laboratory, Imperial College London, London SW7 2BW, United Kingdom.
E-mail address: johann.boucle@unilim.fr (J. Bouclé).

1631-0705/$ – see front matter
doi:10.1016/j.crhy.2007.10.005

1. Introduction

In a context where the development of renewable sources of energy is a major issue, photovoltaic energy conversion appears as a promising alternative to fossil energy, mainly due to non-toxic and non-polluting operation, as well as to an inexhaustible resource. However, although crystalline silicon based solar cells exhibit some of the highest power conversion efficiencies (η), their high production costs, due to high temperature and high vacuum processes, limit their widespread use in the long term. In this context, photovoltaic devices based on organic semiconducting materials take advantage of low-cost fabrication routes while allowing the development of applications on flexible substrates [1]. Although the dye sensitized photo-electrochemical cell (the 'Grätzel' cell) exhibits the most competitive efficiencies among molecular devices, with η of nearly 11% [2,3], the use of a liquid electrolyte increases the number of processing steps involved, resulting in extensive research towards efficient solid state devices. During the last decade, bulk heterojunction solar cells, based on the junction of electron donor (D) and acceptor (A) semiconductors [4], have been widely investigated, and power conversion efficiencies up to 5% have been obtained for improved polymer/fullerene blends [5]. In this type of solar cell, the light absorbing donor material is combined with a molecular acceptor presenting higher electron affinity which allows exciton dissociation and rapid electron transfer at the D/A interface (see Fig. 1). However, the intrinsic exciton diffusion length associated with organic semiconductors such as π-conjugated polymers or small molecules is of the order of 10 nm and therefore fine control of the active layer morphology at the nanoscale is required. Efficient charge generation thus depends upon the achievement of effective interpenetrated D/A junctions. Furthermore, organic device performances are limited by poor charge transport properties resulting from low charge carrier mobilities on the order of 10^{-6}–10^{-3} $\mathrm{cm^2\,V^{-1}\,s^{-1}}$. The use of organic materials which degrade rapidly under ambient conditions, results also in short device lifetimes, and sealing or encapsulation systems have to be implemented additionally in the device structure.

In this context, hybrid devices based on the use of inorganic semiconducting acceptor materials take advantage of high electron mobilities and high chemical stability [6–8]. Obtained from solution in a wide range of morphology,

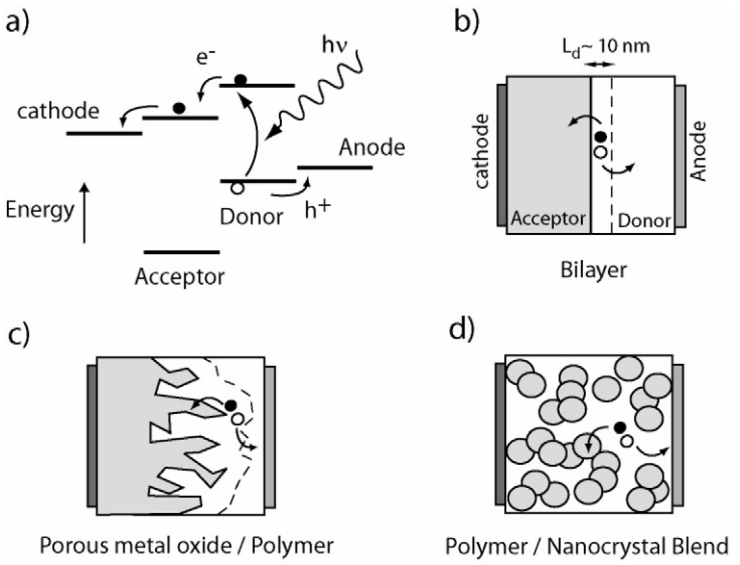

Fig. 1. (a) Flat band diagram of a typical bulk heterojunction solar cell showing exciton formation and dissociation at the donor/acceptor interface. (b) Bilayer device structure where both donor and acceptor material composed a flat junction. The exciton diffusion length (L_d) defines the absorption zone where photogenerated exciton can effectively give rise to separated charge states in both materials. (c) Bulk heterojunction solar cell based on a porous inorganic metal oxide electrode infiltrated by a conjugated donor polymer. (d) Schematic of a polymer/nanocrystal blend device structure.

Fig. 1. (a) Représentation simplifiée de la configuration énergétique d'une cellule à hétérojonction illustrant la génération d'un exciton et sa dissociation à l'interface des matériaux donneurs et accepteurs. (b) Structure d'un composant bicouche où les matériaux donneurs et accepteurs définissent une interface planaire. La longueur de diffusion de l'exciton du matériau donneur (L_d) définit la zone d'absorption optique permettant la dissociation effective des excitons photogénérés en charges libres. (c) Cellules solaires à hétérojonction à base d'une électrode nanoporeuse inorganique infiltrée par un matériau conjugué organique. (d) Structure d'une cellule solaire de type mélange polymère/nanocristaux.

inorganic semiconductors such as TiO_2, ZnO or CdSe, allow a fine control of the active layer morphology when associated with an organic donor material, and can lead to improved device stability and lifetime. Several studies have been devoted to exploit hybrid device geometry using a nanoporous metal oxide electrode infiltrated by a conjugated polymer, or using a nanocrystal/polymer blend approaches (see Fig. 1 for the different device structures). The first approach takes advantage of an improved inorganic network where electrons can find a continuous path to the collecting electrode [9–11]. However, infiltrating a conjugated polymer in a porous network remains the main limitation step towards the achievement of a large D/A interface [12]. For the second approach, the use of a nanocrystal/polymer blend mixture enables the deposition in a single step of thin films where both acceptor and donor can, in principle, be intimately mixed [13,14]. However, fine control of the nanocrystal surface chemistry is required in order to avoid particle aggregation, and blend morphology must be controlled to ensure charge percolation paths for efficient charge separation, transport and collection [15]. In both structures, the main issue remains the achievement of an interpenetrating network of both the inorganic and organic components at the nanoscale, limited by the intrinsic incompatibility of hydrophilic inorganic materials with organic compounds and apolar solvents used in their process.

Inorganic semiconductors used in such devices include II–VI semiconductors and metal oxides. In particular, titanium dioxide (TiO_2) has been widely investigated in dye-sensitized solar cells. Following this approach, solid state hybrid devices based on mesoporous TiO_2 thin films have been deposited and infiltrated with conjugated polymers such as poly(phenylvinylene) derivatives [16], resulting in 40% external quantum efficiency (EQE) and η up to 0.58% under AM1.5 simulated solar illumination (100 mW cm^{-2}) [17]. Promising efficiencies have also been demonstrated using vertically aligned ZnO rods grown on a substrate, which exploit a very high electron mobility and vertical pore structures [18]. Regarding the blend approach, power conversion efficiencies of 1.7% and 1.4% have been respectively demonstrated using CdSe [13] and ZnO [14] nanoparticles in conjugated polymers. Further improvements have been obtained by replacing the nanoparticles with three-dimensional nanocrystals in order to improve electron percolation in the blend. CdSe tetrapods in a poly(p-phenylenvinylene) derivative (OC_1C_{10}-PPV) have thus demonstrated efficiencies as high as 2.1% (AM 1.5, 100 mW cm^{-2}) [19]. The use of a red polyfluorene co-polymer, resulting in an extended spectral response out to 650 nm, resulted in further improvements with η up to 2.4% [20].

This work is devoted to a recent example of hybrid bulk heterojunction solar cells based on the blend of TiO_2 nanoparticles and poly(3-hexylthiophene) (P3HT). Although the highest blend device performance has been obtained using II–VI semiconductor compounds, non-toxic metal oxide nanoparticles have been widely investigated due to their high electron affinity and mobility, and the possibility to easily tune their physical properties from synthetic control. Device efficiencies have been reported recently for blends of isotropic TiO_2 particles with P3HT ($PCE = 0.42\%$, AM1, 100 mW cm^{-2}) [21], and elongated TiO_2 rods in poly[2-methoxy-5-(2′-ethyl-hexyloxy)-1,4-phenylene vinylene] MEH-PPV ($PCE = 0.49\%$, AM1.5, 100 mW cm^{-2}) [22]. In this work, the use of elongated TiO_2 rods with a high mobility polymer such as P3HT aims to exploit improved charge carrier mobilities in both components. The blend morphology, charge transfer properties and device performance will be discussed in order to point out the main parameters controlling the device function: blend morphology, TiO_2 rod surface chemistry, cell structure, etc.

2. Experimental considerations

Nanocrystalline TiO_2 nanorods are synthesised in solution through a non-hydrolytic route [23], using titanium tetraisopropoxide (TIPT) in the presence of amine (surfactant) and trioctylphosphine oxide (TOPO, co-surfactant) in heptadecane. The addition of amine allows the growth of elongated TiO_2 rods rather than isotropic particles [24]. The obtained nanoparticles (7 nm × 19 nm), are found mainly capped with surface TOPO molecules and present a high degree of crystallinity with the main features in the X-ray diffraction patterns being assigned to bulk anatase [25]. Additionally, isotropic TOPO-capped TiO_2 particles (7 nm × 7 nm), prepared using the method described in Ref. [23], and TiO_2 rods capped with oleic acid (OLEA), synthesised as in Ref. [26], will also be incorporated in P3HT for comparison purposes.

The hybrid TiO_2:P3HT blends are processed using a procedure described elsewhere [25]. Briefly, the TOPO- (or OLEA-) capped TiO_2 rods (or isotropic particles) are initially dried and co-dissolved with P3HT (Merck Chemicals) in chloroform (30 mg/ml) in order to achieve TiO_2 loadings ranging from 30 to 70 vol.%. Blend thin films (100–200 nm) are deposited by spin-coating the initial mixture on ITO glass substrates previously coated with 50 nm thick poly-(3,4-ethylenedioxythiophene):poly(styrene sulfonate) (PEDOT:PSS, H.C. Starck, Baytron P) for device preparation, or on spectrosil substrates for the optical characterisation. Metallic top contacts (gold or aluminium depending on the device

polarity, 100 nm thick) are evaporated under vacuum through a shadow mask that defines six devices per substrate each of effective area of 0.042 cm^2. Alternatively to the 'direct polarity' device configuration, ITO/PEDOT:PSS/blend/Al, a 'reverse polarity' geometry, ITO/denseTiO_2/blend/PEDOT:PSS/Au, was also studied, by using dense TiO_2 backing layers (30 nm) deposited by spray pyrolysis from TIPT precursor solutions [27]. All devices presented in this study were annealed at 120 °C under inert atmosphere for 5 minutes, for both the direct and reverse polarities, prior to optical or electrical characterisations.

In some cases, a ligand exchange procedure is applied to the TOPO-capped TiO_2 rods in order to replace the insulating TOPO molecules by the amphiphilic ruthenium dye cis-bis(isothiocyanato) (2,2′-bipyridyl-4,4′-dicarboxylato) (2,2′-bipyridyl-4,4′-di-nonyl) ruthenium(II) (Z907, Solaronix SA). To this end, the dried TOPO-capped nc-TiO_2 nanorods are initially dispersed in chloroform (200 mg/ml) and the suspension is co-dissolved in presence of an excess of the Z907 molecules for 96 h at 50 °C. The Z907-capped nanorods are extracted by adding an excess of *n*-hexane in the mixture to precipitate the modified particles. The final product, recovered after centrifugation and drying steps, is easily re-dispersed in chloroform at 30 mg/ml for the blend preparation with P3HT.

Transmission electron microscopy (TEM) was performed to elucidate the morphology of the rods initially dispersed in chloroform and deposited on a copper observation grid (FEI Philips Tecnai 20, 120 kV). Atomic force microscopy (AFM) topography images were recorded in non-contact mode (tapping mode) on a Burleigh Metris 2000 microscope.

Both photoluminescence quenching (FluroroMax 3.0 spectrofluorometer, excitation at 520 nm) and microsecond–millisecond transient absorption spectroscopy (TAS, experimental configuration described in Ref. [28]) were used to elucidate the charge transfer properties of the blend films. For TAS, the excitation (nitrogen-pumped dye laser, repetition rate ∼4 Hz, pulse duration <1 ns) was set to 520 nm with a pump energy density of 45 $\mu J\,cm^{-2}\,pulse^{-1}$ and the probe wavelength (tungsten lamp) was chosen at 950 nm, where the P3HT polaron photoinduced absorption signal is strong.

The device J–V characteristics were recorded under inert atmosphere and at room temperature using a computer-controlled Keithley 237 source measure unit, in the dark and under simulated AM1.5 solar irradiance at either 100, 50 or 40 $mW\,cm^{-2}$ (Tungsten lamp, Oriel).

3. Results and discussion

3.1. Influence of the particle surface ligand and aggregation on blend morphology

Fig. 2(a) presents a TEM picture corresponding to the TOPO-capped TiO_2 rods. From these observations, the mean rod diameter and length are estimated to 7 and 19 nm respectively. The AFM pictures corresponding to TiO_2:P3HT blends incorporating TOPO-capped TiO_2 rods is presented Fig. 2(b). Fig. 2(c) corresponds to a P3HT blend incorporating isotropic TOPO-capped particles, and Fig. 2(d) is associated with OLEA-capped TiO_2 rods incorporated in P3HT.

Particle aggregation is shown for the blends based on isotropic TOPO-capped particles and rods capped with OLEA. This observation demonstrates the influence of both the particle morphology and surface ligand on the rheological behaviour of TiO_2 nanocrystals in organic solutions. Smaller isotropic particles were hard to disperse even in the presence of TOPO, probably due to strong intraparticle interactions generated during synthesis. Unlike TOPO for comparable rod dimensions, OLEA seems to prevent efficient particle stabilisation, leading to larger film roughness and to particle aggregation which potentially limit the amount of D/A interface; the unsaturated nature of OLEA may lead to direct binding between surfactant layers. In contrast, the use of TOPO-capped TiO_2 nanorods induces homogeneous blend morphology for all range of concentrations up to a particle content of 70 vol.% (Fig. 2(b)). It is worth noting that blend films presenting strong particle aggregation, such as blends using TOPO-capped particles, can present some discontinuity in the plane of the substrate.

3.2. Charge separation properties in the hybrid TiO_2:P3HT blends

The charge transfer properties of the hybrid blends can be monitored by photoluminescence quenching and transient absorption spectroscopy (TAS). While the first technique gives preliminary evidence of non-radiative decay of photogenerated excitons, the second method can give qualitative and quantitative information on both charge separation yields and recombination kinetics of free charges created across the D/A interface. Fig. 3(a) and (b) presents

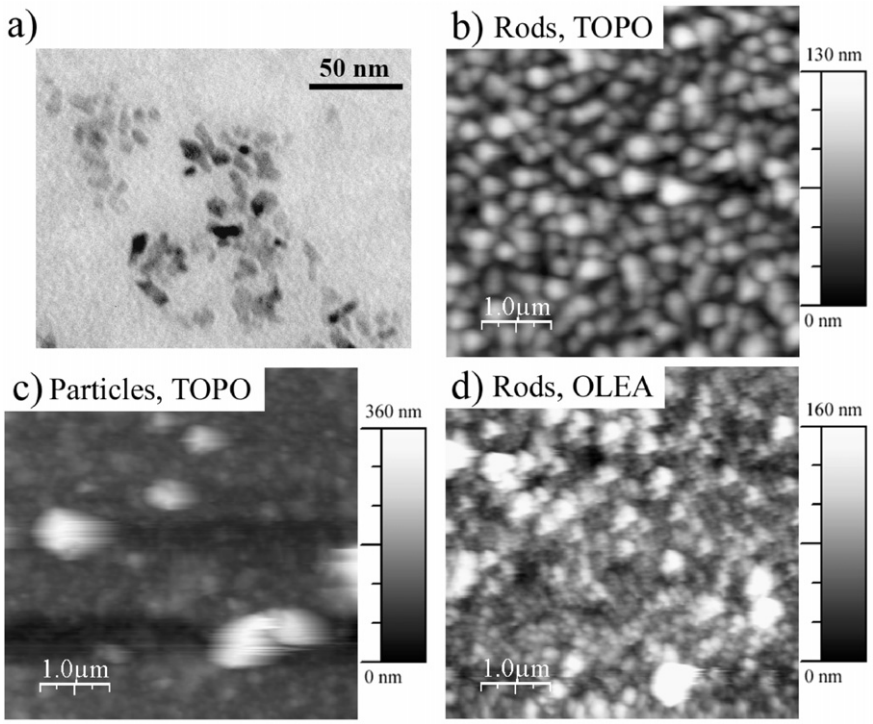

Fig. 2. (a) TEM picture of TOPO-capped TiO_2 rods grown by non-hydrolytic route. Particle mean dimensions are 7 nm diameter and 19 nm length. (b), (c) and (d) present AFM pictures of hybrid blends based on P3HT incorporated with 70 vol.% of: (b) TOPO-capped TiO_2 rods; (c) isotropic TOPO-capped TiO_2 particles (7 nm × 7 nm); and (d) OLEA-capped TiO_2 rods (6 nm × 50 nm).

Fig. 2. (a) Image MET de nanofils de TiO_2 synthétisés par voie non-hydrolytique en solution en présence de la molécule de TOPO comme surfactant. Les dimensions moyennes des particules sont estimées à 7 nm (diamètre) et 19 nm (longueur). Les (b), (c) et (d) presentent les images par AFM des mélanges hybrids TiO_2:P3HT incorporant 70 vol.% de : (b) nanofils de TiO_2 associés au surfactant TOPO ; (b) nanoparticules sphériques de TiO_2 associées au surfactant TOPO ; et (d) nanofils de TiO_2 associés au surfactant OLEA.

the optical absorption and PL spectra of P3HT:TiO_2 blends films containing different amounts of the TOPO-capped TiO_2 rods. PL quenching is evidenced when TiO_2 rods are incorporated in the blend, and increases further as the rod concentration increases in the blend up to 70 vol.%. This observation seems to indicate efficient exciton dissociation followed by rapid electron transfer from the P3HT phase to the metal oxide particles.

Fig. 3(c) presents the TAS signals measured for blends incorporating 70 vol.% of TiO_2 particles of three different types: TOPO-capped TiO_2 isotropic particles, rods and OLEA-capped TiO_2 rods. A significant transient signal is evidenced for the blend based on the TOPO-capped rods ($\Delta O.D. = 3 \times 10^{-4}$) following photo-excitation of the polymer phase at 520 nm, indicating the presence of long-lived photogenerated charges with a half life time of 100 µs. As no change in absorbance was observed in pristine P3HT in these experimental conditions, the decay of the signal can be assigned to recombination of P3HT hole polarons with electrons in the TiO_2 at the D/A interface following exciton dissociation. Regarding the amplitude of the signal, and considering that both the photogenerated electron in the TiO_2 and the positive polaron in P3HT contribute to the TAS signal [25], this observation is consistent with a significant charge separation process in the hybrid blends based on the TOPO-capped TiO_2 nanorods. Both the use of TOPO-capped particles and OLEA-capped rods lead to lower signal amplitude. This observation is consistent with the morphology of the blend films which exhibit particle aggregation when using isotropic nanocrystals with TOPO, or oleic acid as surfactant (see Fig. 2). The achievement of homogeneous particle dispersion in P3HT when using TOPO-capped TiO_2 rods is at the origin of a strong charge separation yield, resulting from high D/A interface. Moreover, the observation that excitation conditions from the top surface or the substrate side of an optically thick film result in similar TAS signal amplitude indicates a rather homogeneous particle dispersion in P3HT over the entire film thickness (insert of Fig. 5(b)).

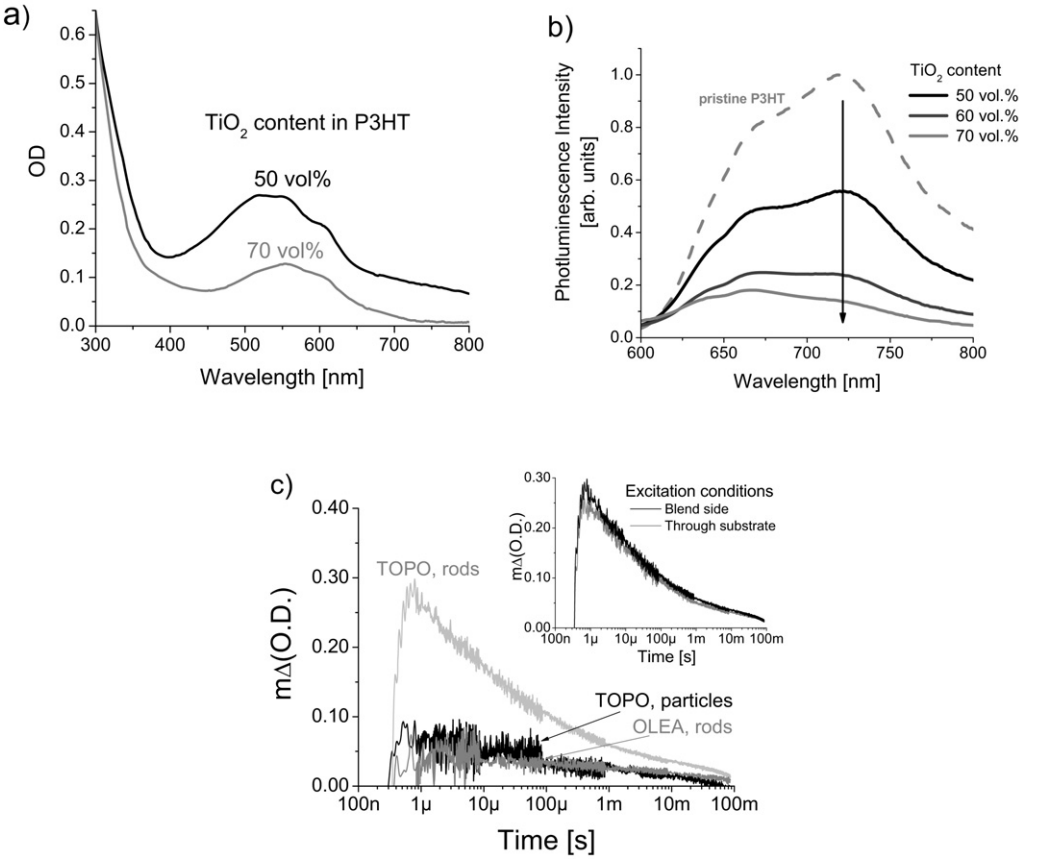

Fig. 3. (a) Optical absorption spectra of blend films based on TOPO-capped TiO_2 particles and P3HT at different particle contents. (b) Photoluminescence spectra of pristine P3HT and hybrid blends based on TOPO-capped TiO_2 rods at different particle concentration. Excitation is performed at 520 nm. (c) Transient absorption signals of hybrid TiO_2:P3HT blends incorporating 70 vol.% of either TOPO-capped TiO_2 particles or rods, as well as OLEA-capped TiO_2 rods. The inset presents the TAS signals corresponding to excitation conditions from the blend side or through the spectrosil substrate. In both graphs, excitation is performed at 520 nm with a power density of 45 mJ cm^{-2} pulse^{-1}, and the probe wavelength is set at 950 nm.

Fig. 3. (a) Spectres d'absorption optique de films hybrides à base de Nanofils de TiO_2 enrobés par la molécule TOPO et de P3HT pour différentes concentrations en particules. (b) Spectres de photoluminescence d'un film de P3HT et de films minces hybrides à base de P3HT et de nanofils de TiO_2 enrobés par la molécule TOPO pour différentes concentrations en particules. L'excitation lumineuse est effectuée à 520 nm. (c) Spectres d'absorption résolus en temps de films mélanges hybrides incorporant 70 vol.% de nanofils de TiO_2(TOPO), de nanoparticules isotropes de TiO_2(TOPO), et de nanofils de TiO_2(OLEA). En insert, les spectres associés à une excitation du coté du film mélange et à travers le substrat de spectrosil sont présentés pour le mélange à base de P3HT et de nanofils de TiO_2(TOPO). L'excitation lumineuse est effectuée à 520 nm (45 mJ cm^{-2} pulse^{-1}), et la longueur d'onde de sonde est fixée à 950 nm.

3.3. Photovoltaic properties of the blends

The photovoltaic performance of the hybrid blends based on TOPO-capped isotropic or rod-like particles in P3HT (70 vol.%) are presented, Fig. 4(a). Improved performance is evidence, in terms of both short circuit current density J_{SC} and open-circuit voltage V_{OC}, for devices based on rods (7 nm × 19 nm) relative to those based on isotropic particles (7 nm × 7 nm).

This result illustrates the influence of both the intrinsic D/A interface and particle morphology on photocurrent generation and device function. Particle aggregation is responsible for a reduction in the donor/acceptor interface area, leading to limited charge separation, hence photocurrent generation. The presence of large particle clusters and aggregates induces also the presence of leakage currents, which can partly explain the low V_{OC} of 210 mV for the device based on isotropic particles compared to 420 mV for the device based on rod-like TiO_2 particles. Such reductions are generally observed in blend devices, where continuous pathways exist for either charge between both electrodes,

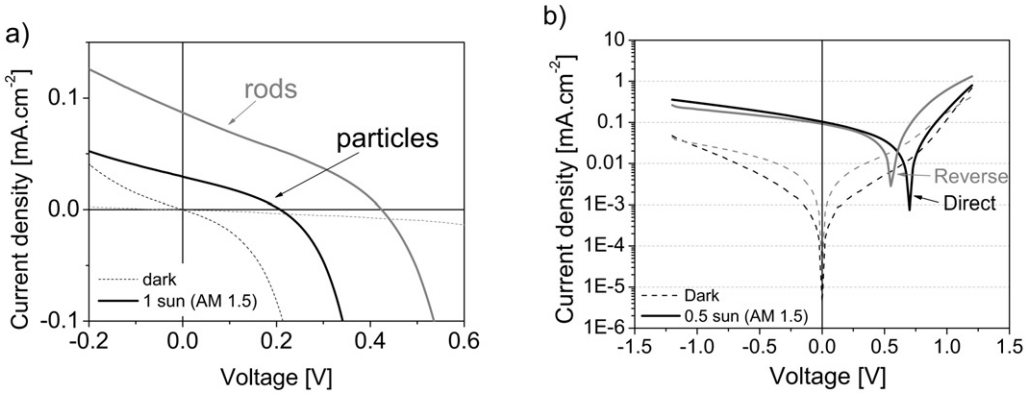

Fig. 4. (a) Current–voltage characteristics of hybrid solar cells based on P3HT and TOPO-capped isotropic (black line) and rod-like (grey line) TiO_2 particles. The particle content is 70 vol.% in both cases. The characteristics are recorded in the dark and under simulated solar spectrum (AM 1.5, 100 mW cm^{-2}). (b) Current–voltage characteristics in a log scale associated with improved P3HT:TiO_2 blend (TOPO-capped rods, 60 vol.%) devices in both direct (ITO/PEDOT:PSS/blend/Al, black line) and reverse polarity (ITO/denseTiO_2/blend/PEDOT:PSS/Au, grey line). The characteristics are recorded in the dark and under simulated solar irradiation (AM 1.5, 50 mW cm^{-2}).

Fig. 4. (a) Caractéristiques courant–tension des cellules mélanges à base de P3HT et de particules de TiO_2 (TOPO) sphériques (courbe noire) et allongées (courbe grise). La concentration en particules est de 70 vol.% dans les deux cas. Les courbes ont été obtenues dans le noir et sous spectre solaire simulé (AM 1,5, 100 mW cm^{-2}). (b) Caractéristiques courant–tension en représentation semi-logarithmique associées à une cellule mélange P3HT incorporant 60 vol.% de nanofils de TiO_2 (TOPO) en configuration de polarité directe (ITO/PEDOT:PSS/mélange/Al, courbe noire) et inverse (ITO/TiO_2 dense/mélange/PEDOT:PSS/Au, courbe grise). Les courbes ont été obtenues dans le noir et sous irradiation solaire simulé (AM 1,5, 50 mW cm^{-2}).

compared to bilayer structures where each electrode is contacted only with one material [19]. Particle morphology may also influence device performance through its effect on charge transport, since the use of elongated rods compared to isotropic particles can limit the number of hopping events required for electrons to reach the cathode [13]. Additionally, some influence from differences in particle surface chemistry between the isotropic particles, which are synthesised with TOPO only as surfactant, and the rods, which use TOPO and amine as co-surfactants, may be present.

Other experimental parameters, such as the blend composition and device annealing have been investigated in order to improve the performance of the blend devices based on TOPO-capped TiO_2 nanorods [25]. A low fill factor of 0.28 is evidenced for the cells based on the rod-like particles. Apart from the intrinsic charge mobilities, this low fill factor can result from the relative roughness of the blend films and low shunt resistance. In order to improve the device selectivity, a reverse device configuration can be implemented, by using additional dense TiO_2 layer in a ITO/dense TiO_2/blend/PEDOT:PSS/Au multilayer geometry. Comparing with the direct ITO/PEDOT:PSS/blend/Al configuration where the ITO electrode is used to collect holes, this reverse geometry uses the dense TiO_2 and PEDOT:PSS layers as hole and electron blocking layers respectively, resulting in improved device selectivity. The reverse polarity was indeed found useful for the improvement of performance of hybrid devices based on conjugated polymers and porous metal oxide electrode such as TiO_2 [17] or ZnO [18]. The current–voltage characteristics of blend devices based on P3HT and TOPO-capped TiO_2 nanorods (60 vol.%) are presented in Fig. 4(b) for the direct and reverse device polarities. Although a lower shunt resistance is associated with the reverse polarity, a slight increase of the fill factor up to 0.31 illustrates the effect of improved device selectivity. However, a lower open-circuit voltage is evidenced in the reverse (550 mV) compared to the direct (700 mV) polarity. Part of this difference is explained through the additional contribution to the D/A interface of the dense TiO_2 layer. Where only the TiO_2 nanorod/P3HT interface controls the device function in the direct polarity, this additional interface could decrease the effective photovoltage in the reverse geometry due to a lower TiO_2 conduction band edge in the dense than in the nanostructured TiO_2. An additional reduction of V_{OC} may also arise from the presence of leakage currents in the reverse geometry.

As promising as the P3HT/TiO_2 blend approach appears, the main limitation to device performance, either in the direct or reverse polarity, remains a poor photocurrent in the order of 0.1 mA cm^{-2}, resulting in power conversion efficiencies of only $\eta = 0.03\%$ under simulated AM 1.5 conditions (100 mW cm^{-2}). The presence of organic insulating molecules at the particle surface, such as TOPO, could be at the origin of such limitations by preventing efficient

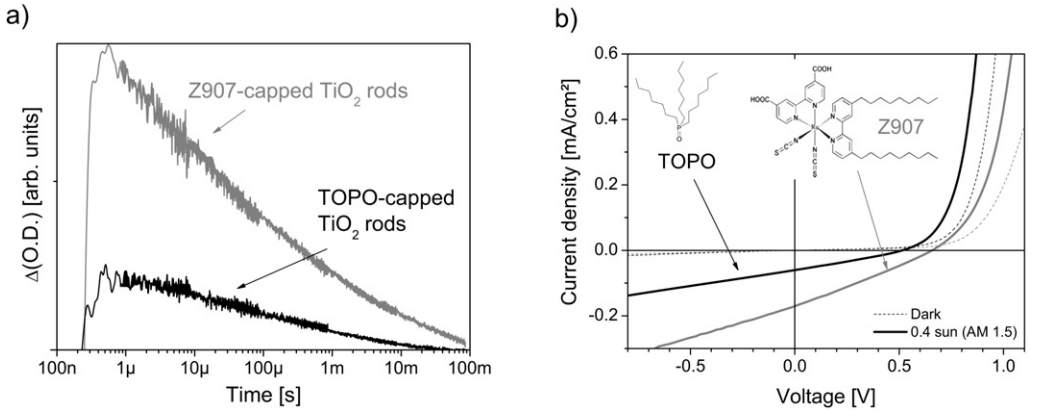

Fig. 5. (a) TAS signals corresponding to hybrid blend devices based on P3HT and either TOPO- (black line) or Z907- (grey line) capped TiO_2 nanorods (60 vol.%), before or after ligand exchange procedure respectively. Excitation is performed at 520 nm with a power density of 45 mJ cm^{-2} pulse^{-1}, and the probe wavelength is set at 950 nm. (b) Current–voltage characteristics of the corresponding devices (direct polarity) in the dark and under simulated solar irradiation (AM 1.5, 40 mW cm^{-2}). The chemical structure of TOPO and Z907 are represented as insets.

Fig. 5. (a) Spectres TAS associés aux films minces mélanges à base de P3HT et de nanofils de TiO_2 (60 vol.%) avant (enrobés de TOPO, courbe noire) et après (enrobés de Z907, courbe grise) la procédure d'échange de ligands. (b) Caractéristiques courant–tension des cellules solaires correspondantes (polarité directe) dans le noir et sous illumination solaire simulée (AM 1,5, 40 mW cm^{-2}).

charge dissociation at the interface and by reducing interparticle electron hopping rates [15]. In order to better adapt the particle surface chemistry to charge separation and transport, ligand exchange procedures are carried out in order to replace the insulating TOPO molecules by the ruthenium dye complex Z907 at the particle surface (see experimental part and Ref. [25] for further details). Fig. 5(a) presents the TAS signals corresponding to both TOPO- and Z907-capped TiO_2:P3HT blends.

A strong increase of the signal amplitude is shown, indicating improved charge separation yield after the ligand exchange procedure with Z907. The corresponding device characteristics (Fig. 5(b)) show higher device performance in terms of V_{OC}, J_{SC} and power conversion efficiency ($\eta = 0.07\%$). These observations are consistent with the limiting role of the TOPO molecules as insulating barriers regarding both the interfacial exciton dissociation and interparticle electron transport. However, although the presence of the conjugated Z907 molecules at the metal oxide surface significantly helps electron transfer from P3HT to the TiO_2 network, the photocurrent remains poor considering the effective charge separation yields observed in the blends. Considering the highly dispersive recombination kinetics of charges revealed by TAS, electron traps are likely to prevent efficient charge transport within the hybrid P3HT:TiO_2 blends [25]. The presence of such trap distributions associated either with the polymer phase, with the interface or with the metal oxide rods, are rate limiting for both charge recombination and transport. Unlike blends based on ZnO [29] or CdSe [19] particles where the electron states are delocalised over the entire nanoparticle volume, intrinsic traps at the TiO_2 particle surface or in the volume remain are well known and are likely to be one of the main factors limiting device performance [30,31].

4. Conclusion

Solution processed hybrid bulk-heterojunction solar cells appear as a promising alternative to silicon based devices for low cost photovoltaic energy conversion, by taking advantage of both high electron mobility of inorganic compounds and high absorption coefficients and flexibility of organic semiconductors. The use of well-defined inorganic nanostructures, such as CdSe, ZnO or TiO_2, allows fine control of the donor/acceptor interface at the nanoscale, enabling efficient exciton dissociation and charge transfer processes. In this work, blend devices based on elongated TiO_2 nanorods and P3HT show efficient charge separation yields, mainly controlled through the blend morphology, particle shape and surface chemistry at the interface. In particular, we show that the presence of insulating organic ligands at the particle surface prevents efficient charge separation. Although these limitations can be overcome by ligand exchange using conjugated surfactants such as the amphiphilic Z907 dye, trapping of photogenerated charges remains one of the main limitation for efficient charge transport and power conversion efficiency.

References

[1] S.R. Forrest, Nature 428 (2004) 911.
[2] B. O'Regan, M. Grätzel, Nature 353 (1991) 737.
[3] A. Hagfeldt, M. Grätzel, Acc. Chem. Res. 33 (2000) 269.
[4] J.J.M. Halls, et al., Nature 376 (1995) 498.
[5] W. Ma, et al., Adv. Func. Mater. 15 (2005) 1617.
[6] J. Bouclé, et al., J. Mater. Chem. 17 (April 2007) 3141.
[7] M. Grätzel, MRS Bull. 30 (2005) 23.
[8] K.M. Coakley, MRS Bull. 30 (2005) 37.
[9] A.C. Arango, et al., Adv. Mater. 12 (2000) 1689.
[10] P. Ravirajan, et al., J. Appl. Phys. 95 (2004) 1473.
[11] H. Wang, et al., Appl. Phys. Lett. 87 (2005) 023507.
[12] K.M. Coakley, M.D. McGehee, Appl. Phys. Lett. 83 (2003) 3380.
[13] W.U. Huynh, J.J. Dittmer, A.P. Alivisatos, Science 295 (2002) 2425.
[14] W.J.E. Beek, M.M. Wienk, R.A.J. Janssen, Adv. Mater. 16 (2004) 1009.
[15] N.C. Greenham, X.G. Peng, A.P. Alivisatos, Phys. Rev. B 54 (1996) 17628.
[16] A.C. Arango, et al., Adv. Mater. 12 (2000) 1689.
[17] P. Ravirajan, et al., Appl. Phys. Lett. 86 (2005) 143101.
[18] P. Ravirajan, et al., J. Phys. Chem. B 110 (2006) 7635.
[19] B. Sun, et al., J. Appl. Phys. 97 (2005) 014914.
[20] P. Wang, et al., Nano Lett. 6 (2006) 1789.
[21] C.Y. Kwong, et al., Chem. Phys. Lett. 384 (2004) 372.
[22] T.-W. Zeng, et al., Nanotechnology 17 (2006) 5387.
[23] T.J. Trentler, et al., J. Am. Chem. Soc. 121 (1999) 1613.
[24] S. Chyla, et al., in press.
[25] J. Bouclé, et al., Adv. Func. Mater. (July 2007), in press, adfm.200700280.
[26] P.D. Cozzoli, A. Kornowski, H. Weller, J. Am. Chem. Soc. 125 (2003) 14539.
[27] P. Ravirajan, et al., Adv. Func. Mater. 15 (2005) 609.
[28] Y. Tachibana, et al., J. Phys. Chem. 100 (1996) 20056.
[29] W.J.E. Beek, M.M. Wienk, R.A.J. Janssen, Adv. Func. Mater. 16 (2006) 1112.
[30] N. Kopidakis, et al., Appl. Phys. Lett. 87 (2005) 202106.
[31] K. Zhu, et al., J. Phys. Chem. B 110 (2006) 25174.